

Chrysanolide A, an unprecedented sesquiterpenoid trimer from the flowers of *Chrysanthemum indicum* L^a

Cite this: *RSC Advances*, 2013, 3, 10168

Received 5th December 2012,

Accepted 3rd April 2013

DOI: 10.1039/c3ra23172k

www.rsc.org/advances

Qiong Gu,^{*a} Yaoyao Chen,^b Hui Cui,^a Dane Huang,^a Jingwei Zhou,^a Taizong Wu,^a Yiping Chen,^b Lina Shi^a and Jun Xu^a

Chrysanolide A, a novel guaianolide-type sesquiterpenoid trimer (3), along with its biogenetically related monomer (Chrysanolide B, 1) and dimer (Chrysanolide C, 2), were simultaneously isolated from *Chrysanthemum indicum* L flowers. Their structures and absolute configurations were elucidated via spectroscopic and computational methods. All isolated compounds were evaluated for their anti-HBV activities.

Chrysanthemum indicum L. (Asteraceae), widely distributed in China and the tropics, is commonly used to treat inflammation, hypertension, and cancer.¹ Pharmacological studies and clinical practices have demonstrated that *C. indicum* L. exhibits antioxidant, anti-bacterial, antiviral, and anti-inflammatory features, and also protects the cardiovascular system.² As part of our ongoing program to discover new anti-HBV constituents from varied natural sources,³ the crude *C. indicum* L. ethanol extract was found to have anti-HBV activity, inhibiting HBsAg and HBeAg secretion, with IC₅₀ values of 35.58 and 101.51 μg mL⁻¹, respectively. Further study of this extract led to three new sesquiterpenoid compounds (1–3), of which compound 3 possesses a hitherto unknown trimeric carbon skeleton. The structures of compounds 1–3 were elucidated using a combination of NMR spectroscopy and computational chemistry. Herein, we report on compound 3's isolation and structural elucidation, as well as a possible biogenetic pathway for compound 3. We also provide a biological evaluation of all compounds.

Compound 1 was isolated as a colorless powder with the molecular formula C₁₅H₂₂O₄ on the basis of HRESIMS (*m/z* 265.1437 [M – H][–]), which indicated five degrees of unsaturation. The IR spectrum exhibited absorptions for hydroxyl (3364 cm⁻¹) and carbonyl groups (1762 cm⁻¹). The ¹³C NMR and DEPT spectra revealed 15 signals for three methyls, two methylenes, seven methines, and three quaternary carbons. The ¹H NMR of 1 exhibited signals for three methyls at δ_H 1.88 (3H, s), 1.41 (3H, d, J

= 6.9 Hz), and 1.29 (3H, s), and one typical methine proton at δ_H 3.95 (1H, t, J = 10.2 Hz). The ¹³C NMR spectrum showed signals for three methyls at δ_C 33.2, 17.9, 15.2, one methine at δ_C 81.0, and one carbonyl at δ_C 179.2. These data indicate that compound 1 is a guaianolide-type sesquiterpenoid. Compound 1's NMR data were comparable to those of known compound 11β, 13-dihydro-*epi*-ligustrin,⁴ which was also identified in the present investigation. The differences in NMR data for 1 and 11β, 13-dihydro-*epi*-ligustrin were at C-8, C-7, C-11, and C-13 (Table S1, ESI[†]). Biogenetically, C-7 should be α-oriented. These observed differences suggest that the configurations of C-8 and C-11 were different from that of 11β, 13-dihydro-*epi*-ligustrin. This was confirmed via ROESY experiments (Fig. S1, ESI[†]). In the ROESY spectrum of 1, the correlations between H₅–H₇, H₅–H₁, H₈–H₁₃, and H₆–H₁₄ indicated that the hydroxyl group at C-8 was β-oriented, and that Me-13 was α-oriented. Thus, compound 1's structure was determined as depicted in Fig. 1, and its trivial name is chrysanolide B.

Compound 2 was isolated as a white powder. Its molecular formula is C₃₅H₄₄O₈ according to negative HRESIMS (*m/z* 591.2936 [M – H][–], calcd for C₃₅H₄₃O₈, 591.2952), thus indicating fourteen degrees of unsaturation. The IR spectrum identified carbonyl (1756 cm⁻¹) and double bond (1456 cm⁻¹) groups. The ¹³C NMR and DEPT spectra revealed 35 signals for six methyls, six methylenes, twelve methines, and eleven quaternary carbons; eight double bond carbons and three carbonyls were identified. NMR spectral (Table S2, ESI[†]) data demonstrates that compound 2 is a sesquiterpenoids dimer. The NMR data of compound 2 is similar to the yehuhua lactone's.⁵ This indicates that compound 2 has a disesquiterpenoid unit. The difference between compound 2 and yehuhua lactone is at C-8. In ¹³CMR spectrum, yehuhua lactone's peaks at δ_C 170.5 (C) and 23.5 (CH₃) contrast with compound 2's peaks at δ_C 166.3 (C), 126.5 (C), 143.3 (CH), 20.3 (CH₃) and 16.3 (CH₃) (Table S2, ESI[†]). These differences are due to angeloyl group for compound 2. These differences were confirmed via ¹H-¹H COSY (H-3''/H-4'') and HMBC (H-3'', H-5''/C-1'', H-3'/C-1'', C-2'', C-4'' and H-4''/C-2'') experiments (Fig. S2, ESI[†]). The HMBC correlation between H-8 and H-7 with C-1'' indicates that the angeloyl group is located at C-8. The double bond configura-

^aResearch Center for Drug Discovery & Institute of Human Virology, School of Pharmaceutical Sciences, Sun Yat-Sen University, Guangzhou 510006, P.R. China. E-mail: guqiong@mail.sysu.edu.cn; Fax: +86-20-39943077; Tel: +86-20-39943077

^bGuangxi University of Chinese Medicine, Guangxi 530001, P.R. China

† Electronic supplementary information (ESI) available. See DOI: 10.1039/c3ra23172k

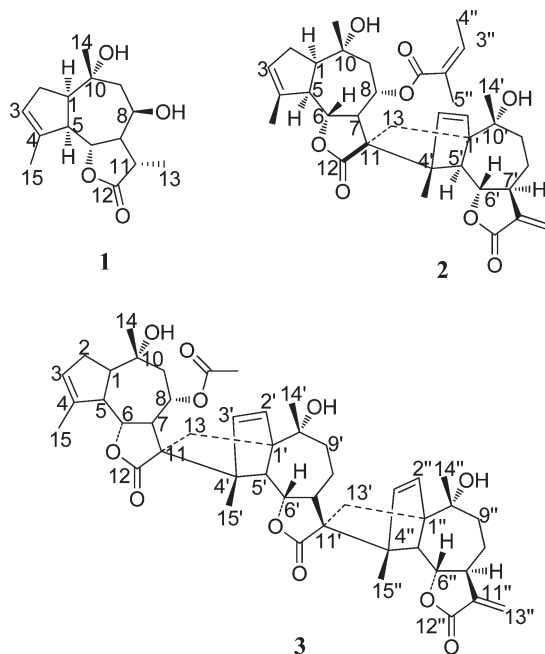


Fig. 1 Structures of compounds 1–3.

tion was confirmed through the key ROESY correlation shown in Fig. S2, ESI†. Accordingly, the structure of compound 2 was assigned as shown in Fig. 1.

Based upon a positive HRESIMS at m/z 821.3969 $[M + Na]^+$, we have assigned compound 3 the formula $C_{47}H_{58}O_{11}$. IR data indicates the presence of carbonyl groups (1750 cm^{-1}), double bonds (1456 cm^{-1}), and hydroxyl groups (3504 cm^{-1}). The EIMS data of compounds 1–3 shows the same fragment peaks at m/z 246, 228, 203, 91, and 83, which indicate that compound 3 has the same scaffold that compounds 1 and 2 have. The ^{13}C NMR and DEPT data of compound 3 exhibited 47 carbons, including one acetyl group (δ_{C} 22.3, δ_{C} 170.9). The ^{13}C NMR data of 3 revealed three sets of signals very similar to those of 1 (Table 1, Table S1, ESI†). On comparing compound 3 with compound 2, with the exception of the angeloyl group signals [δ_{C} 166.3 (C), 126.5 (C), 143.3 (CH), 20.3 (CH_3) and 16.3 (CH_3)], all the resonances observed in the ^1H NMR and ^{13}C NMR of compound 2 were present in compound 3. Compound 3 also has one set of signals [one double bonds (δ_{C} 140.0, 134.4; δ_{H} 5.99, 5.88); two methyls (δ_{C} 29.9, 15.6; δ_{H} 1.14, 1.58); one carbonyl (δ_{C} 179.5); and one methine connected with oxygen (δ_{C} 77.6; δ_{H} 4.00, t, $J = 9.9\text{ Hz}$)], which is characteristic of sesquiterpenoids. The above data suggests that three sets of sesquiterpenoid signals are included in compound 3. In the EIMS spectrum, fragment peaks at m/z 228 $[246 - \text{H}_2\text{O}]^+$, 246, 263 $[306 - \text{CH}_3\text{CO}]^+$, 288 $[306 - \text{H}_2\text{O}]^+$, 306, and 474 $[492 - \text{H}_2\text{O}]^+$, also suggest that compound 3 is a trimeric sesquiterpenoid (Scheme S1, ESI†).

The analysis of COSY, HMBC, and HSQC spectra permitted us to assign all the spectroscopic signals and to propose a planar structure for 3 (Fig. 1). The HMBC spectrum showed correlations of H-2' with C-13, H-3' with C-4' and C-11, and H-13 with C-1'; these correlations support the notion that fragments A and B are connected *via* C–C bonds. Similarly, the correlations of H-13' with

Table 1 Experimental and calculated NMR data for 3 in CDCl_3 (δ in ppm, J in Hz)^a

^1H NMR				^{13}C NMR
No.	Exptl ^b	Calcd	$\Delta\delta^c$	
1	2.53 (1H, dd, 7.8, 17.6)	3.02	0.49	54.6 d
2				33.4 t
3	5.46 (1H, br, s)	5.75	0.29	125.6 d
4				144.2 s
5	2.73 (1H, t-like, 8.2, 9.5)	2.83	0.1	54.1 d
6	3.88 (1H, t, 9.9)	4.65	0.77	78.9 d
7	3.49 (1H, t, 9.2)	2.08	1.41	47.0 d
8	5.33 (m)	4.82	0.51	71.0 d
9				38.5 t
10				73.5 s
11				60.5 s
12				178.8 s
13	1.46 (2H, d, 12.1)	2.04	0.58	36.9 t
14	1.84 (s)	1.85	0.01	18.3 q
15	1.19 (s)	1.33	0.14	33.7 q
1'				64.6 s
2'	5.88 (1H, d, 5.50)	5.84	0.04	134.4 d
3'	5.99 (1H, d, 5.55)	5.92	0.07	140.0 d
4'				56.8 s
5'	2.05 (1H, overlap)	3.4	1.35	66.4 d
6'	4.00 (1H, t, 9.9)	4.12	0.12	77.6 d
7'	2.79 (1H, dd, 9.3, 13.3)	2.87	0.08	44.0 d
8'	1.71 (1H, m)	1.61	0.10	22.4 t
9'	1.87 (1H, m)	2.10	0.23	36.8 t
10'				71.9 s
11'				56.9 s
12'				179.5 s
13'	2.38 (d, 11.8)	2.44	0.06	35.6 t
14'	1.37 (s)	1.23	0.14	15.6 q
15'	1.25 (s)	1.32	0.07	29.9 q
1''				64.4 s
2''	5.85 (1H, d, 5.50)	6.53	0.68	133.7 d
3''	6.26 (1H, d, 5.50)	6.04	0.22	141.4 d
4''				57.8 s
5''	2.21 (1H, overlap)	3.80	1.59	65.9 d
6''	4.14 (1H, t, 9.6)	3.77	0.37	80.2 d
7''	3.18 (1H, m)	2.66	0.52	43.6 d
8''	1.46 (2H, m, overlap)	1.52	0.06	23.6 t
9''				38.4 t
10''				73.2 s
11''				141.2 s
12''				170.6 s
13''	6.07 (1H, d, 3.4); 5.34 (1H, d, 3.4)	6.30 5.67	0.23 0.33	118.8 t
14''	1.32(s)	1.02	0.3	15.4 q
15''	1.29(s)	1.4	0.11	29.5 q
OAc				170.6 s
OAc	2.11 (3H, s)	2.02	0.09	22.3 q

^a Largest deviation $\Delta\delta = 1.59\text{ ppm}$. ^b In 400 MHz. ^c In 100 MHz. ^d $\Delta\delta = |\delta_{\text{calcd}} - \delta_{\text{exptl}}|$.

C-1'', C-4'', and C-11''; H-2'' with C-13' and C-4''; and H-3'' with C-11' reveal that fragment B and C are connected (Fig. 2).

The relative configuration of compound 3 was determined through ROESY spectra analyses (Fig. 3). The ROESY correlations of H-1/H-5, H-6/H-8 and H-15 suggest that 15- CH_3 and 8- CH_3CO are in the β -orientation and α -orientation, respectively. The correlations of H-7/H-13, H-2'/H-14', H-7'/H-13', H-14''/H-2'', and H-6''/H-15'' further support the relative configuration of compound 3 as shown in Fig. 3.

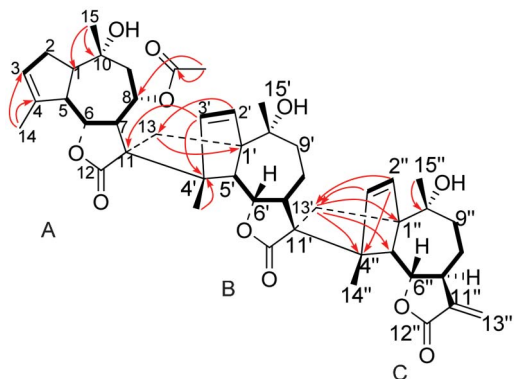


Fig. 2 ^1H - ^1H COSY (bold) and key HMBC (arrows) correlations of **3**.

To further confirm the structure of compound **3**, we calculated the theoretical ^1H NMR spectra of **3** *via* density functional theory (DFT) in Gaussian 09,⁶ as we failed to obtain a single crystal of compound **3**. A conformational initial optimization was first performed at the HF/6-31G level in the gas phase using Gaussian 09. The corresponding minimum geometries were fully optimized at the B3LYP/6-31+G(d,p) level in the gas phase to get more accurate conformers. The ^1H NMR shielding constants of compound **3** were computed using the GIAO technique at the B3LYP/6-31+G(2d,p) level for O in the PCM solvent continuum model (with chloroform as the solvent).⁷ The largest deviation and the average error (CMAD) were only 1.59 and 0.37 ppm, respectively. These results are consistent with the structure deduced from the 1D and 2D NMR experiments.

The electronic circular dichroism (ECD) of compound **3** was also calculated using the Gaussian 09 program at the TD-DFT-B3LYP/6-31 (d, p) level in chloroform. This calculation agreed with the CD spectrum data (Fig. 4). Thus, the absolute configuration of **3** was unambiguously determined as depicted in Fig. 1. It is noteworthy that this is the first guaiane sesquiterpenoid trimer discovered in nature.

A plausible biogenetic pathway for compound **3** is proposed in Scheme 1. Compound **3** may be generated from compound **1**.⁴ Intermediate A, the epimer of compound **1** at C-8, could be converted to intermediate B (cumambrin A) through acetylation.

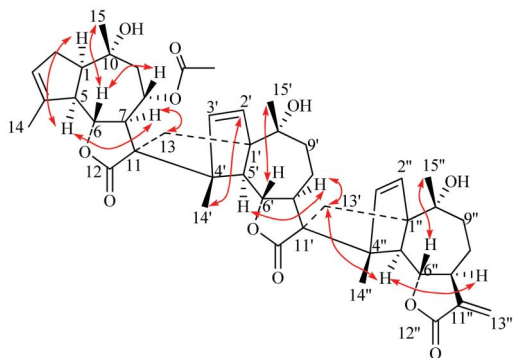


Fig. 3 Selected ROESY correlations (double arrows) of **3**.

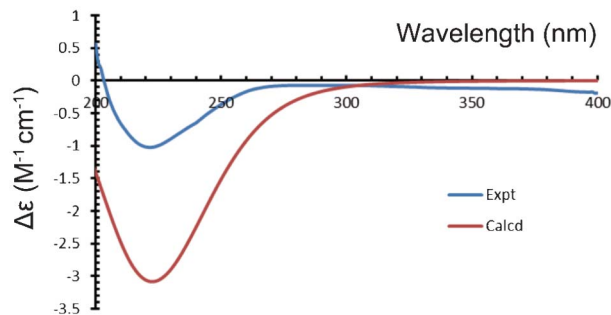
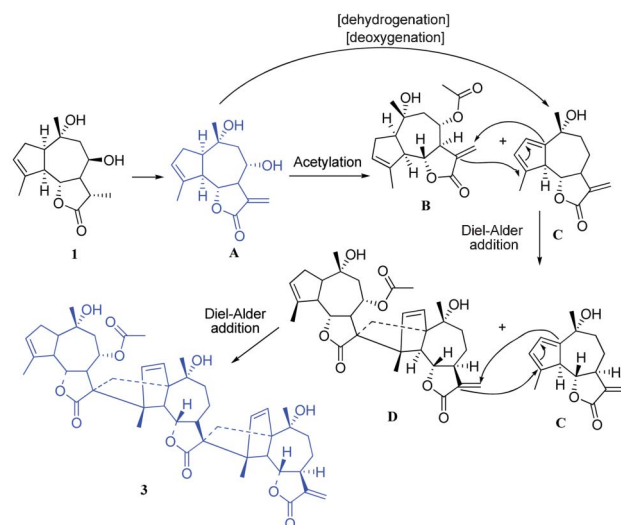


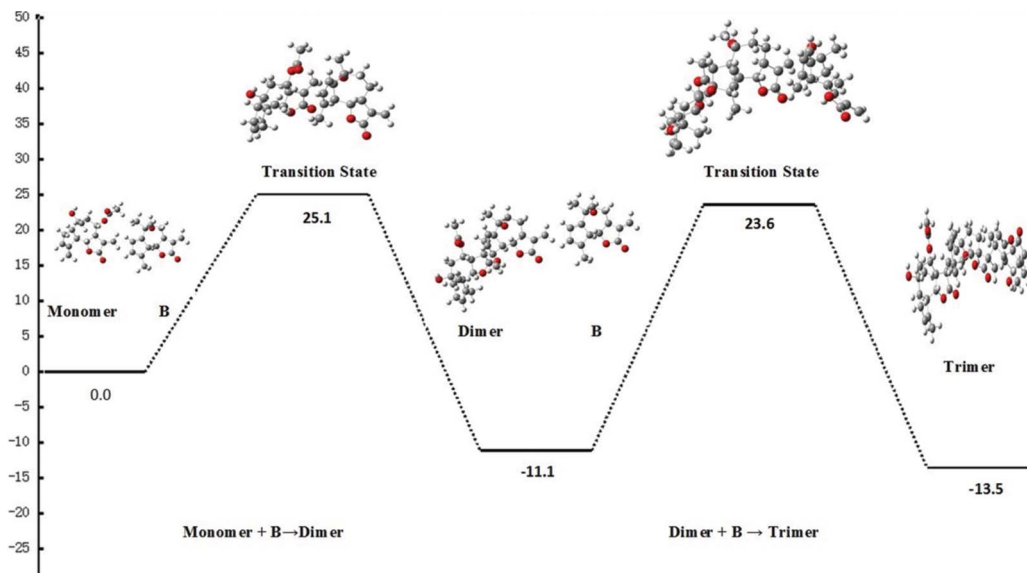
Fig. 4 Experimental and calculated CD spectrum of **3**.

Intermediate C can be derived from intermediate A through dehydration and dehydroxylation. The dimer D (yejuhua lactone) can be generated from the intermediates B and C through a Diels-Alder reaction. The trimer compound **3** can be produced from intermediates D and C by another Diels-Alder cycloaddition reaction.

To the best of our knowledge, compound **3** is the third guaianolid-type sesquiterpenoid trimer isolated from nature.⁸ Interestingly, compounds **1**–**2**, the precursors of compound **3**, were also isolated from the same plant. This further confirms the feasibility of our proposed biogenetic pathway. Moreover, calculated transition state energies (using Gaussian 09, Scheme 2, for detailed procedures see ESI) indicate that the trimer is thermodynamically more stable. The free energy differences between monomer and dimer and between the dimer and trimer are both less than zero (they are $-11.1\text{ kcal mol}^{-1}$ and $-2.4\text{ kcal mol}^{-1}$, respectively). Thus, it is feasible to transform from monomer to dimer, and from dimer to trimer. However, because the free energy difference between dimer and trimer is only $-2.4\text{ kcal mol}^{-1}$, a dimer can form into a trimer only with difficulty. In contrast, the activation energy from reactant monomer to product dimer is close to $20.0\text{ kcal mol}^{-1}$ ($25.1\text{ kcal mol}^{-1}$), which is easy



Scheme 1 Plausible biogenetic pathway of **3**.



Scheme 2 Transition state from monomer (1) to trimer (3) at the M062X/6-31+G(d) level (kcal mol^{-1}) with $\text{eps} = 4$.

to overcome. Unfortunately, the activation energy from reactant dimer to product trimer is far more than $20.0 \text{ kcal mol}^{-1}$ ($34.7 \text{ kcal mol}^{-1}$), making the activation energy hard to conquer. However, the activation energy is still less than 40 kcal mol^{-1} , which means it is just difficult to overcome but not impossible. Thus, these experiments indicate that the trimer is difficult to form and obtain, therefore explaining why the trimer is so rare. Sesquiterpenoids monomers and dimers are widely distributed in the family Asteraceae, and have been used as chemotaxonomic markers.⁹ However, trimeric sesquiterpenoids are rare.

Guaianolide sesquiterpenoids dimer frequently possess both cyclopentadiene and α -methylene butenolide moieties. They are mainly formed *via* enzymatically catalyzed Diels–Alder or hetero-Diels–Alder reactions.¹⁰ Thus, the isolation of compound 3 demonstrates the stunning ability of nature to achieve biodiversity by uniting three sesquiterpenoid moieties *via* two Diels–Alder reactions.

Finally, the anti-HBV activities of compounds 1–3 were assayed in the HepG 2.2.15 cell line, and 3TC (lamivudine, a frequently used clinical anti-HBV agent) was used as the positive control.^{3a} Compounds 1–3 exhibited potent inhibitory activities against the secretion of HBsAg ($\text{IC}_{50} = 131.28, 33.91$ and $6.67 \mu\text{M}$) and HBeAg

($\text{IC}_{50} = 144.48, 30.09$ and $6.23 \mu\text{M}$), respectively. More interestingly the anti-HBV activities increased with the increasing degree of aggregation (Table 2).

In conclusion, we present one unique sesquiterpenoid trimer (Chrysanolide A, 3), together with its biogenetically related monomer (Chrysanolide B, 1) and dimer (Chrysanolide C, 2). As we all known, sesquiterpenoid monomers and dimers are widely distributed, whereas the trimer is really rare in natural products. Compound 3 is third guaianolide-type sesquiterpenoid trimer found in plant kingdom. The existence of 3 suggested that the possibility of further polymerization of sesquiterpenoids in plants.

This work was funded in part by the National Science and Technology Major Project of China (2010ZX09102-305), the National High-Tech R&D Program of China (863 Program) (2012AA020307), the R&D team program of Guangdong Province (NO.2009010058), the National Natural Science Foundation of China (No. 81001372, 81173470) and the External Cooperation Program of the Chinese Academy of Sciences (No.P2010-KF08).

References

- (a) E. Jr. Middleton, C. Kandaswami and T. C. Theoharides, *Pharmacology*, 2000, **52**, 673; (b) W. Cheng, J. Li and T. You, *J. Ethnopharmacol.*, 2005, **101**, 334; (c) S. Jin, P. Zhu and X. Qin, *Pharmacol Clin Chin Mat Med*, 2005, **21**, 39.
- (a) L. D. Kong, Y. Cai and W. W. Huang, *J. Ethnopharmacol.*, 2000, **73**, 199; (b) T. Akihisa, H. Tokuda and E. Ichiishi, *Cancer Lett.*, 2001, **173**, 9; (c) J. Yanez, V. Vicente and M. Alcaraz, *Nutr. Cancer*, 2004, **49**, 191; (d) K. H. Park, M. S. Yang and M. K. Park, *Fitoterapia*, 2009, **80**, 54.
- For selected examples, see: (a) C. A. Geng, X. M. Zhang and Y. M. Zhang, *Tetrahedron Lett.*, 2010, **51**, 2483; (b) C. A. Geng, Z. Y. Jiang and Y. B. Ma, *Org. Lett.*, 2009, **11**, 4120; (c) M. H. Yan, P. Cheng and Z. Y. Jiang, *J. Nat. Prod.*, 2008, **71**, 760; (d) Q. Gu, R. R. Wang and X. M. Zhang, *Planta Med.*, 2007, **73**, 279; (e) R.

Table 2 Anti-HBV activities of compounds 1–3

No.	CC_{50}^b	HBsAg/ μM		HBeAg/ μM	
		IC_{50}	SI	IC_{50}^c	SI^d
1	200.00	131.28	1.52	144.48	1.52
2	32.34	33.91	0.95	30.09	1.07
3	7.89	6.67	1.18	6.23	1.27
3TC ^a	24.8	14.85	1.67	42.36	0.58

^a 3TC positive control. ^b CC_{50} , 50% cytotoxicity concentration. ^c IC_{50} , 50% effective concentration. ^d $\text{SI} = \text{CC}_{50}/\text{IC}_{50}$.

- R. Wang, Q. Gu and L. M. Yang, *J. Ethnopharmacol.*, 2006, **105**, 269.
- 4 C. Zdero, F. Bohlmann and M. Müller, *Phytochemistry*, 1987, **26**, 2763.
- 5 (a) Z. N. Chen and P. J. Xu, *Acta Pharmaceutica Sinica*, 1987, **22**, 67; (b) S. H. Lee, H. K. Kim and J. M. Seo, *J. Org. Chem.*, 2002, **67**, 7670.
- 6 *Gaussian 09, revision B0.1*, Gaussian, Inc., www.gaussian.com.
- 7 (a) M. W. Lodewyk, M. R. Siebert and D. J. Tantillo, *Chem. Rev.*, 2012, **112**, 1839; (b) Y. Q. Ding, X. C. Li and D. Ferreira, *J. Nat. Prod.*, 2009, **72**, 327; (c) C. Diedrich and S. Grimme, *J. Phys. Chem. A*, 2003, **107**, 2524.
- 8 Y. Wang, Y. H. Shen and H. Z. Jin, *Org. Lett.*, 2008, **10**, 5517.
- 9 M. F. Braulio, *Nat. Prod. Rep.*, 2009, **26**, 1125.
- 10 (a) Z. J. Zhan, Y. M. Ying and L. F. Ma, *Nat. Prod. Rep.*, 2011, **28**, 594; (b) H. Oikawa and T. Tokiwano, *Nat. Prod. Rep.*, 2004, **21**, 321.